THE ASTROPHYSICAL JOURNAL, 436:144–151, 1994 November 20

PROBING THE INTERSTELLAR MEDIUM WITH PULSARS ON AU SCALES

DALE A. FRAIL
National Radio Astronomy Observatory, Socorro, NM 87801
JOEL M. WEISBERG
Carleton College, Department of Physics and Astronomy, Northfield, MN 55057
JAMES M. CORDES
Cornell University, Astronomy Department, Ithaca, NY 14853
AND
COREY MATHERS[1]
Carleton College, Department of Physics and Astronomy, Northfield, MN 55057
Received 1994 March 31; accepted 1994 May 13

ABSTRACT

We present a new technique, multiepoch observations of 21 cm absorption against high-velocity pulsars, to probe the properties of the cold neutral hydrogen gas (H I) in the interstellar medium (ISM) at AU scales. In three epochs, over a 1.7 yr interval, we find evidence for significant opacity variations toward all of the pulsars in our sample. Small-scale structure in the ISM is detected on a range of scales from 5 AU to 100 AU, over a wide range of distances (50–2600 pc), opacities ($\tau_{max} = 0.1$–2.5) and directions (anticenter, interarm, high latitude, and local ISM). It appears that small-scale structure is a general property of the ISM and is not confined to special lines of sight. A significant fraction (10%–15%) of the cold H I gas is in this form. These opacity variations do not show any strong correlations with such parameters as transverse distance or integrated opacity, and there is no obvious relation between these structures and those seen in the ionized phase of the ISM.

Subject headings: ISM: abundances — pulsars: general — radio lines: ISM

1. INTRODUCTION

After 40 yr the 21 cm line of neutral hydrogen (H I) continues to be a useful tracer of Galactic structure. The entire Galaxy has been well-studied in H I emission with single-dish telescopes on angular scales of about a degree (Burton 1988; Heiles 1984) revealing the large-scale structure of the Galaxy, including spiral structure, shells, "worms," high-velocity clouds, etc. Select regions studied at arcminute resolution with connected element interferometers (e.g., Green 1989) show that the seemingly smooth and ubiquitous H I gas is composed of multiple arcs, sheets, or filaments. Angular scales on the order of an arcsecond can be sampled by H I absorption measurements made against bright continuum background sources (e.g., Crovisier, Dickey, & Kazès 1985). While these observations cannot map the distribution of H I in detail on these scales, variations are seen in the opacity of the cold atomic gas along closely separated lines of sight and this is ascribed to small-scale structure in the interstellar medium (ISM).

The single most important conclusion to draw from these studies is that the H I gas in our Galaxy is organized on, and maintains, a hierarchy of scales from 1 kpc down to at least 1 pc. Such a statement has important ramifications for the topology of the gas and by extension the processes which produce this hierarchy (Scalo 1985). For many years now there has been both observational and theoretical support for a minimum size scale of approximately 1 pc. Structures on scales smaller than this are not thought to be common in the ISM. Dickey & Lockman (1990) have summarized the many arguments for accepting this statement and conclude that while small-scale structure in the atomic medium does exist, it is only a tiny fraction of the total hydrogen column density along any line of sight.

Diamond et al. (1989) found exciting evidence to the contrary, confirming an earlier detection by Dieter, Welch, & Romney (1976). Both groups had made H I absorption observations against extragalactic sources with the technique of very long baseline interferometry (VLBI). This technique measures angular structure at milliarcsecond resolution, far smaller than the angular scales probed by previous single-dish or connected-element interferometer studies. They detected significant opacity variations over a linear distance of 10^{-4} pc or 20 AU. This is three orders of magnitude smaller than any previously detected structure in the cold atomic gas. Similarly, Frail et al. (1991) noted a large opacity variation toward the pulsar PSR 1821+05 over a period of only 1 yr, while Deshpande et al. (1992) presented evidence for opacity variations toward PSR 1557−50 over a 4 yr timescale. It is difficult to understand how these neutral structures are formed and survive in the ISM. The atomic medium may resemble the diffuse ionized component of the interstellar medium for which many observations suggest a power-law distribution of sizes from 10^7 cm to greater than 10^{14} cm (Cordes et al. 1991). Likewise the AU-sized structures may only be peripherally related to the larger scale structure of the neutral gas, representing a physically distinct population of structures.

In this paper we outline a new approach for studying small-scale structure in the cold atomic phase of the ISM. Using this method we independently confirm the opacity variations seen with VLBI by Diamond et al. on AU scales. We describe the method and outline our observations and reductions in § 2. A

[1] Now at University of Iowa, Department of Physics and Astronomy, Iowa City, IA 52242.

summary of the results for each pulsar is given in § 3, while in § 4 we discuss these results.

2. OBSERVATIONS AND REDUCTIONS

Pulsars are nearly ideal sources for the study of small-scale structure in the H I gas. The compact nature of pulsars allows us to sample the gas with an effective absorption "beam" that is limited only by interstellar scattering (Dickey et al. 1981). In practice, this gives a resolution of typically 0.1–1 mas. The pulsed, periodic nature of pulsars also allows one to correct for the H I emission in the telescope beam exactly, which would otherwise complicate the interpretation of the spectrum. In addition to their small solid angles and their pulsed nature we know that pulsars have transverse velocities of hundreds of km s^{-1}. A pulsar moving at 100 km s^{-1} through the ISM traverses 20 AU yr^{-1}. This unique combination of properties means that by monitoring temporal variations in the H I opacity of the gas along the line to a pulsar we are able to probe the structure of this gas on AU scales.

The range of angular and linear scale sizes that a pulsar can probe is determined by three factors: the pulsar's velocity with respect to the gas, its distance from the observer, and its scatter broadening diameter. This is illustrated schematically in Figure 1. One can see immediately that the full resolution available from this technique has yet to be utilized. For most pulsars in this sample an angular resolution of less than 1 mas is attainable, probing structure at sub-AU scales.

We chose a total of seven pulsars to observe, spanning a range of distances in largely random directions through the Galaxy. All were chosen because they are sufficiently bright at 1.42 GHz to obtain a high signal-to-noise spectrum. Table 1 lists our pulsars along with the relevant data on each. Columns (2)–(4) are the galactic longitude, latitude, and dispersion measure, respectively. Except for PSR 1737+13, the distances in column (5) and transverse velocities in column (6) are from the compilation of interferometric observations by Harrison, Lyne, & Anderson (1993). For PSR 1737+13 we quote the scintillation velocity measurement from Cordes (1986). For convenience, in column (7) we list the transverse distance traveled by the pulsar in 1 yr as calculated from the velocity in column (6).

TABLE 1

OBSERVED PULSARS

Pulsar (1)	l (2)	b (3)	DM (pc cm^{-3}) (4)	D (pc) (5)	V_t (km s^{-1}) (6)	$\dot{\Omega}$ (AU yr^{-1}) (7)
0540+23.....	184.4	−3.3	77.6	2646	288	60
0823+26.....	197.0	31.7	19.5	375	192	40
0950+08.....	228.9	43.7	3.0	130	35	7
1133+16.....	241.9	69.2	4.8	155	274	58
1737+13.....	37.1	21.7	48.9	1800	144	30
1929+10.....	47.4	−3.9	3.2	55	21	4
2016+28.....	68.1	−4.0	14.2	1300	39	8

The observations were made on three occasions, 1990 April, 1990 November, and 1991 December with the 305 m Arecibo telescope. The time interval between adjacent observations is 0.65 yr and 1.05 yr. For PSR 2016+28 a prior observation had been made in 1987 February, 3.13 yr before the start of this program. The observing procedure and reduction process was identical to that detailed by Clifton et al. (1988) and Frail et al. (1991). In short, the pulsars were observed in the 21 cm line with a 1.25 MHz bandwidth and 512 frequency channels (0.5 km s^{-1} per channel). The pulsar period was split into 64 intervals, and an independent spectrum was gathered for each of the 64 pulsar phase intervals during each integration time (10 minutes). This two-dimensional array of data in pulse phase versus frequency was processed to form the final absorption and emission spectrum toward the pulsar.

As it was our intention to compare spectra made on several observing sessions over a long period of time, extra effort was taken to assure that variations in the spectra, if any, were real. To check the frequency stability of the primary and secondary local oscillators, a transmitter was turned on at the end of each day and observed in the regular manner. Data which showed a displacement of this line from its expected

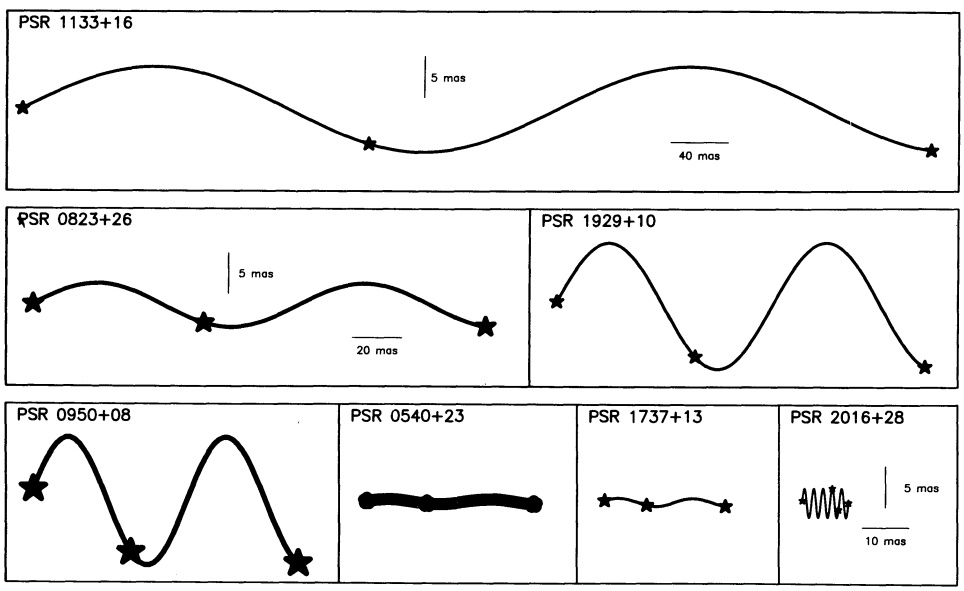

FIG. 1.—A schematic representation of the angular motion of each pulsar on the sky. The angular displacement is given by the length of each sinusoidal segment. The height of the sinusoid is proportional to the annual parallax and the width of each line is proportional to the expected scatter broadening diameter. The epochs of observation are indicated by the filled symbols. The phase of the sinusoid is arbitrary, assigned to be zero on the first epoch. The largest proper motion is that of PSR 1133+16 at 371 mas yr^{-1}. The largest annual parallax is that of PSR 1929+10 at 18 mas. The largest angular broadening is that of PSR 0540+23 at 1 mas.

spectral channel were discarded. This behavior was seen on only one observing session, after a telescope maintenance period. During postprocessing further tests were made to check assumptions about bandpass calibration, zenith angle effects, polarization, and signal-to-noise weighting. The 70–150 spectra taken toward each pulsar on a single epoch were subdivided into two sets according to one of the criteria given above, and the final weighted absorption spectra from each were compared. No significant differences between these spectra were seen, for example, between right and left polarization, between low and high signal-to-noise spectra, and between low and high zenith angle data. In addition, no signficant bandpass variations were detected over our observing interval.

Two additional effects had to be removed from some of our data before any quantitative analysis could begin: scintillation and emission ghosts. The scintillation bandwidth of PSR 0540+23 at 1.42 GHz is 0.3 MHz, sufficiently small to introduce unwelcome frequency structure across our narrow 1.25 MHz band (Cordes, Weisberg, & Boriakoff 1985). In this case the continuum was not determined by the usual means (i.e., fitting a constant level outside the region of absorption), but was fitted instead with a 20th order cosine polynomial. We also saw small modulations in the bandpass in the absorption spectra of PSR 2016+28 (whose scintillation bandwidth at 1.42 GHz is approximately 20 MHz). No significant improvement in the final baseline level was achieved for PSR 2016+28 or any other of the pulsars by performing the polynomial fit instead of the usual straight line fit.

Emission "ghosts" are false images of the emission spectrum that contaminate the absorption spectrum of strong, time-variable pulsars. Weisberg, Rankin, & Boriakoff (1980) were the first to describe the formation of these emission ghosts and outline a method for their removal. In a three-level, two-bit autocorrelator such as that used in this experiment, the zero lag channel is a measure of the total power. However, since we accumulate autocorrelation products for several thousand pulsar periods, the total power is but an average over our integration time (10 minutes). Strong individual pulses can greatly exceed the threshold settings for the samplers and fall outside the linear region of the three-level correction (Kulkarni & Heiles 1980). This slight distortion appears in the spectrum as a faint, inverted version of the emission spectrum. Typically the "ghost" was a 1–3 σ feature, seen only for the two strongest pulsars PSR 0950+08 and PSR 1929+10, but on one epoch for PSR 1929+10 it was as large as 12 σ. We corrected for the emission ghosts by a method very similar to that used by Weisberg et al. (1980) and Weisberg (1978), estimating the fractional contribution of the emission spectrum to the absorption spectrum for PSR 0950+08 and PSR 1929+10 by a least-squares fit, minimizing the residuals between the emission and the absorption spectrum, and taking care to estimate the true zero level.

3. RESULTS

We present our data in two different formats. The absorption spectra for each epoch are displayed in Figure 2. The spectrum for PSR 0950+08 is not shown since there is no

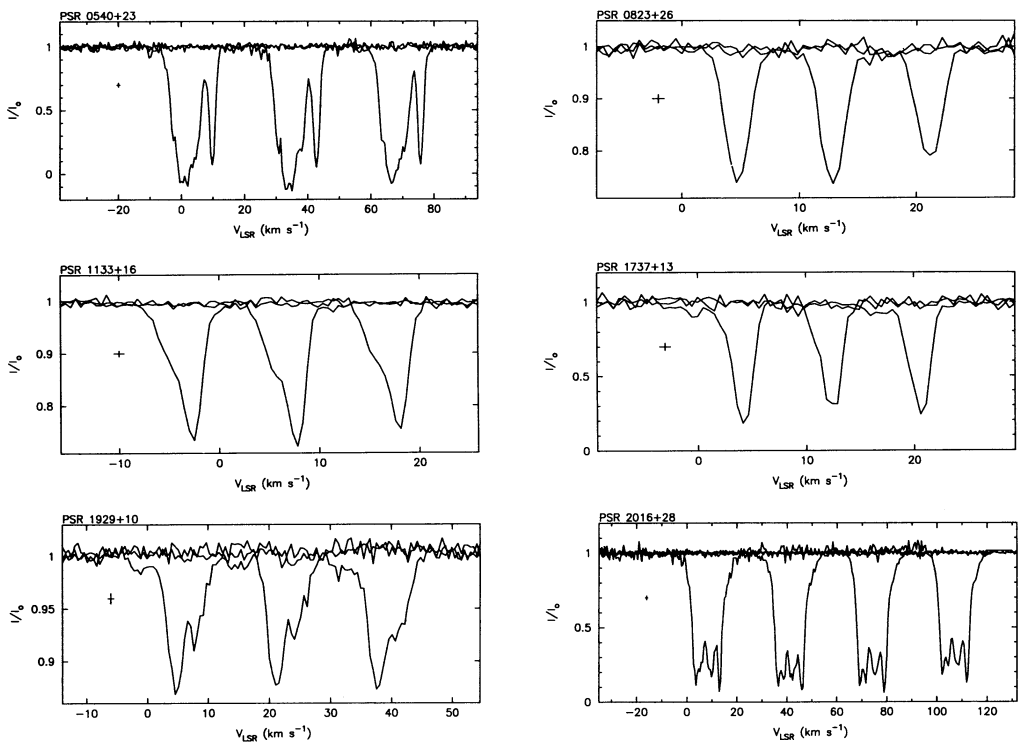

FIG. 2.—Normalized H I absorption spectra made toward six pulsars at several different epochs. The leftmost spectrum in each plot (epoch 1) has the correct velocity scale, but subsequent spectra are shifted to the right by a fixed velocity increment. The time intervals between adjacent epochs is 0.65 yr and 1.05 yr, except for PSR 2016+28 where it is 3.13 yr, 0.65 yr, and 1.05 yr. The length of the plus in the vertical direction indicates the rms noise level ($\pm\sigma_\tau$) in the optical depth spectrum, determined at velocities away from H I emission. Bright H I emission adds to the system temperature, increasing the rms noise in the absorption profile. Typically this increases the rms noise within the line by no more than a factor of 1.5. In the case of PSR 2016+28 and PSR 0540+23 the rms noise at the deepest parts of the line are a factor of 2–3 times that shown by the plus. The length of the plus in the horizontal direction indicates the channel resolution, which is $\pm$0.5 km s^{-1} in all cases.

detectable absorption down to an rms level in the optical depth of 0.005. This is consistent with observations showing a local minimum in the H I column density in this direction (Paresce 1984), and with the work of Phillips & Clegg (1992), who conclude that a significant fraction of the path length to PSR 0950+08 is through the local bubble of hot, X-ray emitting gas. Figure 3 shows the mean absorption profile toward each pulsar and beneath these are the difference spectra between epochs. We begin with a discussion of these data on a source-by-source basis.

PSR 0540+23.—A relatively high velocity pulsar in the Galactic anticenter direction. Because of velocity crowding in this direction, the H I emission brightness temperature reaches a peak value of 120 K (Weisberg et al. 1980). As a consequence, there is an increased noise temperature and increased noise in the spectrum at the absorption line velocities. Hence the pulsar intensity at these velocities drops below zero, making an accurate measure of the opacity for several of the deep lines nearly impossible. Despite this difficulty there are clear signs of significant opacity variations above the noise. It is also worth noting in this multicomponent profile that similar variation do *not* occur at all velocities and at all epochs. This would be the case if the variations were an artifact of the calibration process. Instead, between any two epochs opacity variations are detected in some line components but not others. This temporal behavior strongly indicates that the variations are real and are not an artifact of the calibration process.

PSR 0823+26.—This is one of four high-latitude pulsars in our sample and of great interest because it is known to exhibit strong refraction events that are believed to be caused by discrete, AU-sized ionized structures in the ISM (Clegg, Fiedler, & Cordes 1993). The absorption spectrum toward PSR 0823+26 consists of a single, narrow feature (Dickey et al. 1981). There is little or no change between the first and second epochs but between the second and third epochs the peak optical depth changes from $\tau = 0.31$ to $\tau = 0.24$, a 6 σ variation.

PSR 1133+16.—This pulsar has the highest proper motion in our sample. There are at least two distinct absorption features in the spectrum toward PSR 1133+16 at -3 and -5 km s^{-1} (Dickey et al. 1981), and perhaps a much weaker feature near $+1$ km s^{-1}. The profiles are remarkably similar from one epoch to the next, with the largest variation coming from the -3 km s^{-1} feature between epoch 2 and epoch 3, where the peak optical depth decreases from $\tau = 0.32$ to $\tau = 0.28$, a 5 σ variation.

PSR 1737+13.—The absorption spectrum toward this pulsar is a blend of at least two features at $+4$ km s^{-1} and $+2.6$ km s^{-1} (Weisberg, Rankin, & Boriakoff 1987). There is a third, weak line at -0.5 km s^{-1} with $\tau = 0.1$ that disappears at epoch 2 only to reappear again at epoch 3. The largest variation occurs between epoch 1 and 2 in the $+4$ km s^{-1} feature, where the peak optical depth decreases from $\tau = 1.7$ to $\tau = 1.2$.

PSR 1929+10.—The absorption spectrum toward PSR 1929+10 has three distinct components at $+8$ km s^{-1}, $+4.5$ km s^{-1}, and a broad, weak feature at -1 km s^{-1}. The largest variations in opacity occur near the $+8.0$ km s^{-1} line. It is somewhat surprising perhaps to detect cold H I gas in absorp-

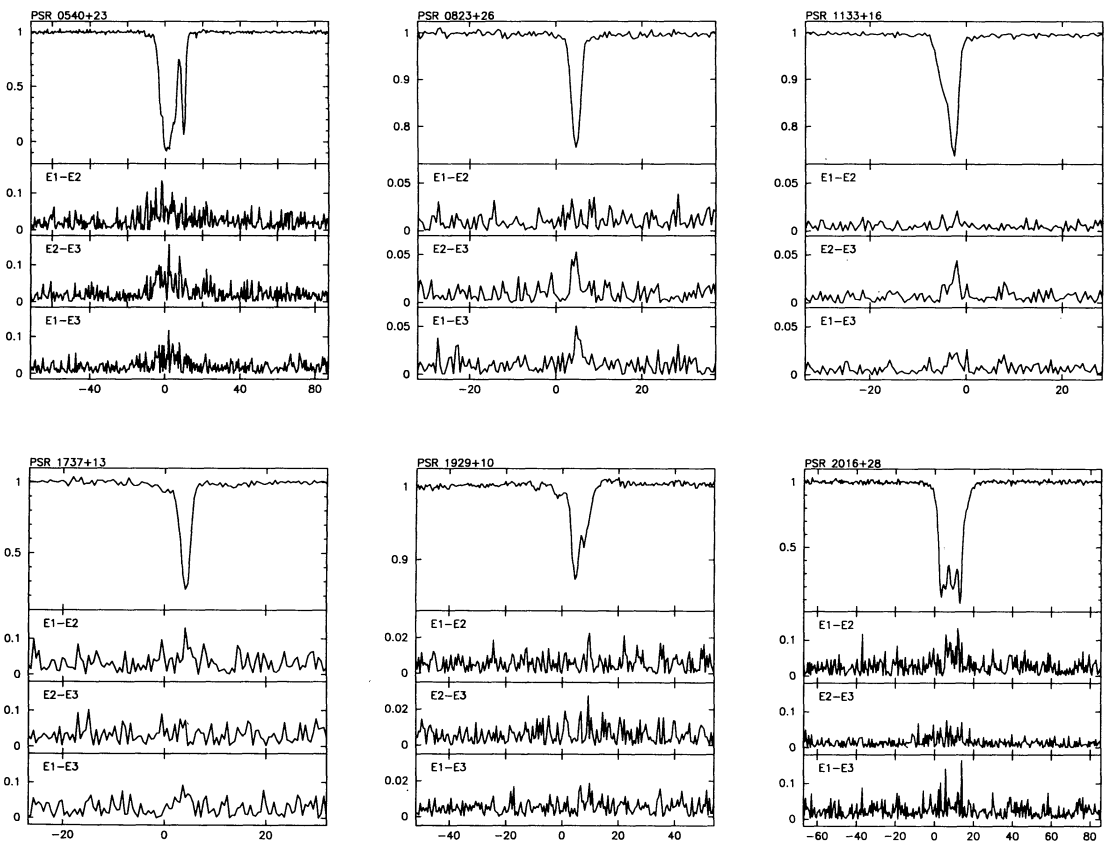

FIG. 3.—Mean H I absorption profiles and difference profiles made toward six pulsars. The mean profile is formed from the average of the absorption profiles over all the three epochs (four epochs for PSR 2016+28). The difference spectra show the absolute value of the changes in relative intensity (I/I_0) between epochs.

tion against this nearby pulsar (Weisberg et al. 1980). However, the radius of the local bubble along the plane is only 30–60 pc (Cox & Reynolds 1987) and hence it is likely that the distance to PSR 1929+10 is larger than the DM-based value of 55 pc given in Table 1. The H I column density of the absorbing gas toward PSR 1929+10 is approximately 2×10^{20} cm^{-2} (see § 4.1), implying a distance to the pulsar of 100 pc (Paresce 1984).

PSR 2016+28.—A lower than average line-of-sight density in both the atomic and ionized gas, plus a low degree of interstellar scattering (Frail 1989; Cordes et al. 1985) convincingly demonstrates that this pulsar lies in the interarm region between the Perseus and the Sagittarius arms. There are four observing epochs for this pulsar, giving a total time between the first and last epochs of 4.8 yr. The first epoch for PSR 2016+28 is from 1987 February, taken from an identical experiment by Clifton et al. (1988). The multicomponent profile shows significant changes in one or more spectral features from one epoch to the next. Epoch 4 is unusual in that *all* spectral lines show changes in their depth. Such an change could be produced by an error in the data reduction by, say, an incorrect normalization. All data from each epoch were reduced in exactly the same way and a close inspection of the data showed nothing unusual about the fourth epoch data for PSR 2016+28.

In summary, we find evidence for significant opacity variations toward all six of the pulsars in our sample. Small-scale structure in the ISM appear to exist on a range of scales from 5 AU to 100 AU. We confirm the VLBI results of Diamond et al. (1989) and Dieter et al. (1976) using a completely independent approach. We emphasize that we have sampled several random lines of sight, with a range of opacities ($\tau_{max} = 0.1$–2.5), distances, and directions. Variations are seen in the anticenter direction, an interarm region, at high latitudes, and in the local ISM. It appears that small-scale structure is a general property of the ISM and not confined to special lines of sight. We proceed in § 4 to attempt to quantify the amplitude of these fluctuations in the neutral medium and to understand their relation with other phases of the ISM.

4. DISCUSSION

4.1. *Integrated Profile Variations*

For convenience we define the "*equivalent width*" EW, which is simply the integrated optical depth,

$$\mathrm{EW} = \int \tau \, dv \,, \tag{1}$$

expressed in units of km s^{-1}. The column density of the cold neutral gas along the line of sight is related to EW by

$$N_{\mathrm{H\,I}} = 1.82 \times 10^{18} \langle 1/T_s \rangle^{-1} \mathrm{EW} \,, \tag{2}$$

where $\langle 1/T_s \rangle^{-1}$ is the harmonically weighted spin temperature along the path, whose value in the plane is typically 50–100 K (Kulkarni & Heiles 1988). The EW was measured from each spectrum, and a mean absorption measured $\overline{\mathrm{EW}}$ was derived by averaging over all epochs. The changes in EW from one epoch to the next are designated at δEW. They represent real changes in the column density of the cold neutral gas as the pulsar moves through the ISM. These data are shown in Figure 4 for all pulsars in our sample. While there are additional absorption spectra for our pulsars in the literature (e.g., Dickey et al. 1981), we have not used them, in order to avoid any systematic errors introduced when comparing data taken with different observing procedures, different correlators, and different reduction methods.

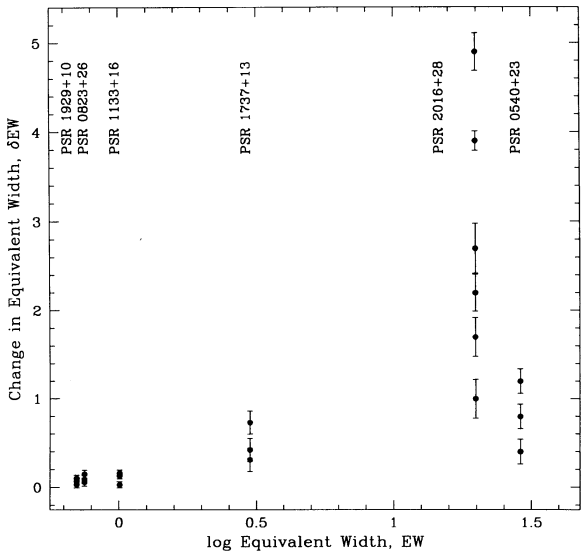

FIG. 4.—The relationship between δEW and $\overline{\mathrm{EW}}$. An approximately linear trend of increasing δEW with $\overline{\mathrm{EW}}$ is apparent.

The smallest signficant column density variation we detected was $(9.3 \pm 3.2) \times 10^{18}$ cm^{-2} (for $T_s = 50$ K) between the second and third epochs toward PSR 1929+10. The largest column density variation of $(4.5 \pm 0.1) \times 10^{20}$ cm^{-2} was toward PSR 2016+28 between the second and fourth epochs. These column density changes are of the same order measured by toward several compact extragalactic radio sources with VLBI by Dieter et al. (1976) and Diamond et al. (1989), who determined $\delta N_{\mathrm{H\,I}}$ of 10^{20} cm^{-2} and 4×10^{19} cm^{-2}, respectively. Marscher, Moore, & Bania (1993) have also measured variations of $\delta N_{\mathrm{H}} = (3$–$7) \times 10^{20}$ toward molecular clouds by monitoring absorption variations in the H_2CO molecule.

The relative importance of this small-scale structure is given by the fractional variation in column density $\delta\mathrm{EW}/\overline{\mathrm{EW}}$. Over our three epochs and six lines of sight $\delta\mathrm{EW}/\overline{\mathrm{EW}}$ spans a range from 0% to 25%. These values are distributed uniformly with a median of 13%. For 3C 147, observed by both Dieter et al. (1976) and Diamond et al. (1989), EW $= 7 \times 10^{20}$ cm^{-2} (Lazareff 1975; Hughes, Thompson, & Colvin 1971), giving $\delta\mathrm{EW}/\overline{\mathrm{EW}} = 14\%$. Evidently a significant fraction (10%–15%) of the total column density of the cold medium is tied up in small-scale structure. We will return to this point in § 4.3.

4.2. *Line Profile Variations*

The absorption spectra also allow us to determine the variations in opacity at different locations along the line of sight to the pulsar. We chose to do our analysis by comparing opacities between corresponding velocity channels from one epoch to the next. This approach is conceptually simple and is free of the uncertainties in the Gaussian fitting of line profiles (Crovisier et al. 1985). However, it contains the assumption that adjacent channels are independent of each other. In the absence of inter-

nal cloud dispersions our 0.5 km s^{-1} resolution represents distances of 100–500 pc between adjacent velocity channels, well in excess of the scale sizes we are probing ($\Delta\Omega_{max} \leq 110$ AU). While cloud-cloud velocity dispersions are of order 7 km s^{-1}, the internal velocity dispersion of individual clouds peaks at 0.75 km s^{-1} (Kulkarni & Heiles 1988). Thus at least in the case of a simple spectrum with well-separated Gaussian components we can treat the channel variations as substructure within an individual cloud.

For each spectrum we must first decide whether a feature in a given channel is significant or not. A feature must exceed a 3 σ noise level to be classed as significant. The noise level determination takes into account the increased noise from channels which have high H I emission brightness temperatures. Saturated opacities ($\tau \gg 1$) were not used in the analysis as they are acutely sensitive to small variations in the noise level. In practice, this resulted in discarding data from only eight of the 32 significant velocity channels of PSR 0540+23, and none in any other pulsar spectra.

Once a valid list of opacities was obtained for each pulsar, differences and means were calculated between epochs. This resulted in a total of 435 mean $\bar{\tau}$ opacities and difference $\delta\tau$ opacities, of which over half (228) were from PSR 2016+28. In Figure 5 we display these data in a statistical way, showing the percentage of $\bar{\tau}$ and $\delta\tau$ values in one of six opacity bins. The largest values of $\bar{\tau}$ and $\delta\tau$ in Figure 5 are predominantly from PSR 2016+28 and PSR 0540+23, the lines of sight with the largest EW values. These large $\delta\tau$ values are from optically thick ($\bar{\tau}$) spectral lines, and so the uncertainty in $\delta\tau$ is of order $\pm$30%. Errors for the weaker lines are considerably smaller (5%–10%). It is apparent from Figure 5 that significant opacity variations are present on a variety of spatial scales from 1 AU to 110 AU.

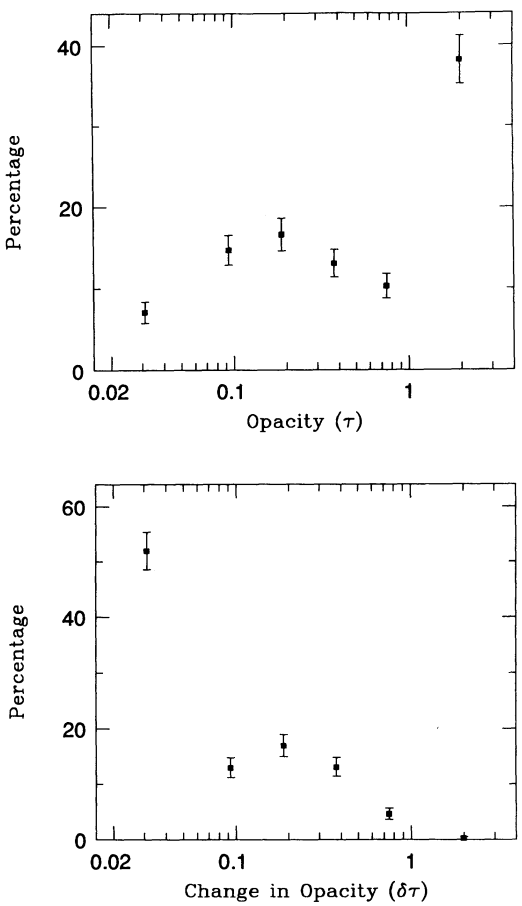

FIG. 5.—The statistical distribution of mean opacities (*top panel*) and difference opacities (*bottom panel*) for all pulsars in our sample.

It would be of considerable interest to determine some measure of the strength of the opacity fluctuations as a function of the scale size sampled in the ISM from one epoch to the next. In general this can be described by a "structure function," $\langle |\tau(x) - \tau(x+\sigma)|^2 \rangle$, where τ is either an integrated opacity, or a individual channel opacity, measured at a location or time x and remeasured at a later time or different transverse distance $x + \sigma$. We attempted to construct temporal structure functions for *individual* pulsars based on comparisons of opacity fluctuations between different velocity channels but found that we had insufficient data to make valid comparisons. This may be possible to do in the future as fortunately, the number of independent $\delta\tau$ values grow by $N(N-1)/2$, where N is the number of epochs. A spatial structure function is difficult to determine in practice because of the difficulties of translating the observed velocities in each spectral bin to a distance for calculating a transverse displacement $\Delta\Omega$. The problem with calculating kinematic distance to individual velocities features in a spectrum are well known (Frail & Weisberg 1990) and are particularly prone to error for nearby pulsars, which form the bulk of our sample.

4.3. *Relation to Previous Studies of Small-Scale Structure*

Small-scale structure in the neutral phase of the ISM has been studied by many different groups. Emission fluctuations in the H I gas on arcminute scales suggest that it is quite smooth (Jahoda et al. 1985; Lockman, Hobbs, & Shull 1986). However, H I emission spectra do not easily distinguish between the cold and warm neutral phases of the ISM and thus the widely distributed warm phase (Kulkarni & Heiles 1988) can "wash out" small-scale structure in the cold gas. H I absorption profiles measured against background radio sources are a better probe of the structure in the cold gas.

Studies at arcminute and arcsecond scales (e.g., Griesen & Liszt 1986; Crovisier et al. 1985; Liszt, Dickey, & Greisen 1982; Schwarz & Wesselius 1978) have revealed opacity variations on parsec and sub-parsec scales. Likewise Langer, Prosser, & Sneden (1990) and Bates et al. (1992, and references therein) see profile variations in the Na I D lines of the closely packed bright giants in globular clusters at the same spatial scales. A common and important result seen in all of these studies is the weakening of the opacity variations below a spatial scale of 1 pc, and the near absence of any variations below 0.2 pc (Crovisier et al. 1985). This result has been widely interpreted as a cutoff in the spectrum of cloud sizes for the atomic gas (Cowie & Songalia 1986). Some variations have been seen on smaller scales, for example, in the *IUE* spectra of the binary star κ CrA (Meyer 1990) and in the time-variability of Ca II K and Na I D lines toward HD 72127 A (Hobbs et al. 1991), but these are unusual lines of sight which traverse known supernova remnants. This apparent size threshold is in marked contrast to studies of the cold molecular gas which shows structure down to the resolution limits of the instruments employed (Falgarone & Pérault 1988; Pound, Bania & Wilson 1990; Wilson & Walmsley 1989).

The discovery of opacity variations in the cold H I gas on spatial scales which are two to three orders of magnitude below the previously established limits comes then as a surprise and needs to be explained. In this paper we have demonstrated that the variations first detected by Dieter et al. (1976) are not confined to a small number of specialized lines of sight and that they are detected on a variety of spatial scales from 5 AU to 100 AU. We have further shown that some 10%–15% of the cold medium is found in these small-scale structures. Whatever these structures are, it appears that they cannot be part of a continuous hierarchy of scales in the H I gas but represent a distinct population. Previous attempts to detect opacity variations between 0.2 pc (40,000 AU) and 100 AU have showed a lack of structure on these scales. Furthermore, the fluctuation spectrum of Figure 5 is not a smooth extrapolation of that seen by Crovisier et al. (1985). If it were, the Crovisier et al. (1985) results would predict a $\delta\tau$ values well below 0.1, whereas about 48% of our $\delta\tau$ measurements exceed this value.

Simple arguments by Dieter et al. (1976) and others give densities for these AU-sized "cloudlets" of 10^5 cm^{-3} $\times$ N^{-1}, where N is the number of such cloudlets along the line of sight. These densities are more typical of those observed in molecular clouds and suggest that this gas is in overpressure with the ambient medium and is probably short-lived (Diamond et al. 1989; Heiles 1993). The opacity fluctuations owe their origin to density variations and perhaps to some degree to temperature and velocity fluctuations.

Cloudlet models, while used as theoretical constructs (Münch 1952; McKee & Ostriker 1977) have been rejected by previous authors (Dickey et al. 1981; Payne, Salpeter, & Terzian 1983). They have argued that the area filling factor of any small-scale structure in the H I gas has to be close to unity. Otherwise the statistical properties of absorbing clouds would differ depending on the angular size of the background continuum source, an effect which is not seen. However, the "beam averaging" that would take place with a population of small structures occupying only 10%–15% of the total column density might easily be absorbed in the scatter of the cloud properties.

4.4. *Relation to the Ionized Phase of the ISM*

One of the more unique properties of pulsars is that they can be used to probe both the cold neutral atomic gas and the ionized gas along identical lines of sight. Monitoring variations in both the equivalent width and the dispersion measure allows us to look for correlations in these fluctuations and to learn something about the relation between the neutral and ionized phases of the interstellar medium.

Recent studies of DM variations have been made by Backer et al. (1993) and Phillips & Wolszczan (1991). In the later case these authors made observations of PSR 0823+26 commensurate with our H I absorption observations between epoch 1 (1990 April) and epoch 2 (1990 November). From Figure 1 of Phillips & Wolszczan (1991) we estimate that the δDM during this interval was +0.0013 pc cm^{-3}. The δEW value over this time was −0.06. Converting these to more easily comparable column densities gives $\delta N_{\rm H+} = 4 \times 10^{15}$ cm^{-2} and $\delta N_{\rm H\,I} = -5.5 \times 10^{18}$ cm^{-2} (for $T_s = 50$ K). The variation in the electron column density is only 0.1% of that seen in the cold gas. In contrast, the total column densities (from DM and EW) toward PSR 0823+26 show that there are roughly equal amounts of cold and ionized gas in this direction. Thus the DM variations are of a much smaller magnitude than the EW variations, and at least in this one instance the variations are anticorrelated. In general, the DM changes in a relatively smooth monotonic way reflecting the fact that the variations in DM are driven by large-scale features onto which are superposed stochastic fluctuations produced by smaller scales. Although the data set is limited, preliminary indications are that the EW variations are not smooth on these same timescales, implying a flatter power spectrum for the EW fluctuations. The present indications are that the EW and DM fluctuations are unrelated.

Alternatively, the opacity variations that we see could be related in some way to the "extreme scattering events" seen by Fielder et al. (1987). These sudden changes in the continuum flux density of extragalactic sources are thought to be due to refractive scintillation from the passage of an AU-sized ionized structure across the line of sight. Romani, Blandford, & Cordes (1987) estimate that the column density for a "typical" event is $N_{\rm H+} = 5 \times 10^{17}$ cm^{-2}, rising to $N_{\rm H+} \simeq 10^{19}$ cm^{-2} for the more dramatic events. While the electron and H I column density variations are of a similar magnitude, it is difficult to reconcile the difference in the event rates for these two processes. According to Fielder et al. (1987) these caustic events happen toward a given extragalactic source only 0.7% of the time. In contrast, we see opacity variations toward *all* of the pulsars in our sample, and in some instances these variations are detected at several locations along the line of sight. If these caustic structures are simply the ionized versions of the H I density structures, then they must dissipate in a very short time to explain their much lower space density.

5. CONCLUSIONS

Multiepoch, 21 cm absorption measurements have been made with the Arecibo 305 m telescope toward seven pulsars for the purpose of detecting small-scale structure in the cold neutral phase of the ISM. Significant opacity variations were detected on all lines of sight on spatial scales of 5–110 AU, confirming earlier VLBI detections. The column density variations we measure range from 10^{19} cm^{-2} to 5×10^{20} cm^{-2}. We estimate that 10%–15% of the cold neutral gas is found in AU-sized structures. The origin of these presumably dense, short-lived structures is unknown. With our limited data set we cannot discern any strong relationship between these fluctuations and other relevant quantities such as distance, total column density, transverse distance, etc., and they do not seem to be related to the warm ionized phase of the ISM. Future observations should be made to these and other pulsars with the aim of better constraining the spatial spectrum of these opacity variations.

D. A. F. acknowledges the financial support of the National Radio Astronomy Observatory through a Jansky Fellowship and the Natural Sciences and Engineering Research Council of Canada through an NSERC Postdoctoral Fellowship. J. M. W. received support from NSF grants AST 89-19061 and AST 92-22435. J. M. C. received support from NASA and the NSF (grant AST 92-18075), as well as from the National Astronomy and Ionosphere Center, which operates the Arecibo Observatory under a cooperative agreement with the NSF. D. A. F. thanks P. Diamond, J. Dickey, M. Goss, and U. Schwartz for useful discussions.

REFERENCES

Backer, D. C., Hamma, S., van Hook, S., & Foster, R. S. 1993, ApJ, 404, 636
Bates, B., Wood, K. D., Catney, M. G., & Gilheany, S. 1992, MNRAS, 254, 221
Burton, W. B. 1988, in Galactic and Extragalactic Radio Astronomy, ed. K. Kellermann & G. L. Verschuur (New York: Springer-Verlag), 295
Clegg, A. W., Fiedler, R. L., & Cordes, J. M. 1993, ApJ, 409, 691
Clifton, T. R., Frail, D. A., Kulkarni, S. R., & Weisberg, J. M. 1988, ApJ, 333, 332
Cordes, J. M. 1986, ApJ, 311, 183
Cordes, J. M., Weisberg, J. M., & Boriakoff, V. 1985, ApJ, 288, 221
Cordes, J. M., Weisberg, J. M., Frail, D. A., Spangler, S. R., & Ryan, M. 1991, Nature, 354, 121
Cowie, L. L., & Songalia, A. 1986, ARA&A, 24, 499
Cox, D. P., & Reynolds, R. J. 1987, ARA&A, 25, 303
Crovisier, J., Dickey, J. M., & Kazès, A. 1985, A&A, 146, 223
Deshpande, A. A., McCulloch, P. M., Radhakrishnan, V., & Anantharamaiah, K. R. 1992, MNRAS, 258, 19P
Diamond, P. J., Goss, W. M., Romney, J. D., Booth, R. S., Kalberla, P. M. W., & Mebold, U. 1989, ApJ, 347, 302
Dickey, J. M., & Lockman, F. J. 1990, ARA&A, 28, 215
Dickey, J. M., Weisberg, J. M., Rankin, J. M., & Boriakoff, V. 1981, A&A, 101, 332
Dieter, N. H., Welch, W. J., & Romney, J. D. 1976, ApJ, 206, L113
Falgorone, E., & Pérault, M. 1988, A&A, 205, L1
Fiedler, R. L., Dennison, B., Johnston, K. J., & Hewish, A. 1987, Nature, 326, 675
Frail, D. A. 1989, Ph.D. thesis, Univ. Toronto
Frail, D. A., Cordes, J. M., Hankins, T. H., & Weisberg, J. M. 1991, ApJ, 382, 168
Frail, D. A., & Weisberg, J. M. 1990, AJ, 100, 743
Green, D. A. 1989, A&AS, 78, 277
Griesen, E. W., & Liszt, H. S. 1986, ApJ, 303, 702
Harrison, P. A., Lyne, A. G., & Anderson, B. 1993, MNRAS, 261, 113
Heiles, C. 1984, ApJS, 55, 585
———. 1993 in Back to the Galaxy, ed. S. S. Holt & F. Verter (New York: AIP), 610
Hobbs, L. M., Ferlet, R., Welty, D. E., & Wallerstein, G. 1991, ApJ, 378, 586
Hughes, M. P., Thompson, A. R., & Colvin, R. S. 1971, ApJS, 23, 323
Jahoda, K., McCammon, D., Dickey, J. M., & Lockman, F. J. 1985, ApJ, 290, 229
Kulkarni, S. R., & Heiles, C. 1980, AJ, 85, 1413
———. 1988, in Galactic and Extragalactic Radio Astronomy, ed. K. Kellermann & G. L. Verschuur (New York: Springer-Verlag), 95
Langer, G. E., Prosser, C. F., & Snedon, C. 1990, AJ, 100, 216
Lazareff, B. 1975, A&A, 42, 25
Liszt, H. S., Dickey, J. M., & Griesen, E. W. 1982, ApJ, 261, 102
Lockman, F. J., Hobbs, L. M., & Shull, J. M. 1986, ApJ, 301, 380
Marscher, A. P., Moore, E. M., & Bania, T. M. 1993, ApJ, 419, L101
McKee, C. F., & Ostriker, J. P. 1977, ApJ, 218, 148
Meyer, D. M. 1990, ApJ, 364, L5
Münch, G. 1952, ApJ, 116, 575
Paresce, F. 1984, AJ, 89, 1022
Payne, H. E., Salpeter, E. E., & Terzian, Y. 1983, ApJ, 272, 540
Phillips, J. A., & Clegg, A. W. 1992, Nature, 360, 137
Phillips, J. A., & Wolszczan, A. 1991, ApJ, 382, L27
Pound, M. W., Bania, T. M., & Wilson, R. W. 1990, ApJ, 351, 165
Romani, R. W., Blandford, R. D., & Cordes, J. M. 1987, Nature, 328, 324
Scalo, J. M. 1985, in Protostars and Planets II, ed. D. C. Black & M. S. Matthews (Tucson: Univ. Arizona Press), 201
Schwarz, U. J., & Wesselius, P. R. 1978, A&A, 64, 97
Weisberg, J. M. 1978, Ph.D. thesis, Univ. Iowa
Weisberg, J. M., Rankin, J. M., & Boriakoff, V. 1980, A&A, 88, 84
———. 1987, A&A, 186, 307
Wilson, T. L., & Walmsley, C. M. 1989, A&AR, 1, 141